



HHS Public Access

Author manuscript

Neurogastroenterol Motil. Author manuscript; available in PMC 2019 October 01.

Published in final edited form as:

Neurogastroenterol Motil. 2018 October ; 30(10): e13380. doi:10.1111/nmo.13380.

Vagus Nerve Stimulation Promotes Gastric Emptying by Increasing Pyloric Opening Measured with Magnetic Resonance Imaging

Kun-Han Lu^{2,4}, Jiayue Cao^{1,4}, Steven Oleson¹, Matthew P Ward^{1,5}, Robert Phillips³, Terry L Powley^{*,3,4}, and Zhongming Liu^{*,1,2,4}

¹Weldon School of Biomedical Engineering, Purdue University, West Lafayette, IN, USA

²School of Electrical and Computer Engineering, Purdue University, West Lafayette, IN, USA

³Department of Psychological Sciences, Purdue University, West Lafayette, IN, USA

⁴Purdue Institute for Integrative Neuroscience, Purdue University, West Lafayette, IN, USA

⁵Indiana University School of Medicine, Indianapolis, IN, USA

Abstract

Background—Vagus nerve stimulation (VNS) is an emerging electroceutical therapy for remedying gastric disorders that are poorly managed by pharmacological treatments and/or dietary changes. Such therapy seems promising since the vagovagal neurocircuitry controlling the enteric nervous system strongly influences gastric functions.

Methods—Here, the modulatory effects of left cervical VNS on gastric emptying in rats was quantified using a 1) feeding protocol in which the animal voluntarily consumed a post-fast, gadolinium-labeled meal and 2) a non-invasive imaging method to measure antral motility, pyloric activity and gastric emptying based on contrast-enhanced magnetic resonance imaging (MRI) and computer-assisted image processing pipelines.

Key Results—VNS significantly accelerated gastric emptying (sham vs. VNS: 29.1±1.5% vs. 40.7±3.9% of meal emptied per 4hrs), caused a greater relaxation of the pyloric sphincter (sham vs. VNS: 1.5±0.1 vs. 2.6±0.4 mm² cross-sectional area of lumen), and increased antral contraction amplitude (sham vs. VNS: 23.3±3.0% vs. 32.5±3.0% occlusion), peristaltic velocity (sham vs. VNS: 0.50±0.02 vs. 0.67±0.03 mm s⁻¹), but not its contraction frequency (sham vs. VNS: 6.1±0.2 vs. 6.4±0.2 contractions per minute, p=0.22). The degree to which VNS relaxed the pylorus was positively correlated with gastric emptying rate (r = 0.5887, p<0.001).

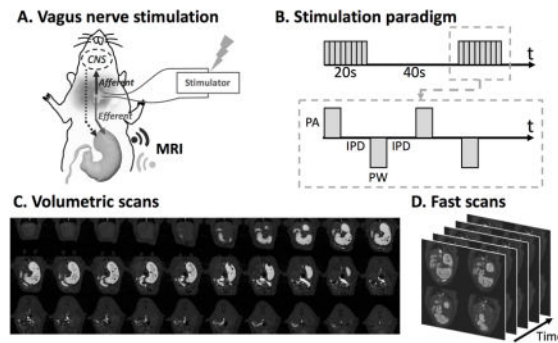
Conclusions & Inferences—The MRI protocol employed in this study is expected to enable advanced preclinical studies to understand stomach pathophysiology and its therapeutics. Results

*Correspondence: Zhongming Liu, PhD, Assistant Professor of Biomedical Engineering, Assistant Professor of Electrical and Computer Engineering College of Engineering, Purdue University, 206 S. Martin Jischke Dr. West Lafayette, IN 47907, USA, Phone: +1 765 496 1872, Fax: +1 765 496 1459, zmliu@purdue.edu. Terry L Powley, PhD, Distinguished Professor of Behavioral Neuroscience, Department of Psychological Sciences, Purdue University, 703 Third Street, West Lafayette, IN 47907, USA, Phone: +1 765 494 6269, powleyt@purdue.edu.
PROFESSOR TERRY POWLEY (Orcid ID : 0000-0001-6689-7058)
DR ZHONGMING LIU (Orcid ID : 0000-0002-8773-4204)

from this study suggest an electroceutical treatment approach for gastric emptying disorders using cervical VNS to control the degree of pyloric sphincter relaxation.

Graphical Abstract

Abbreviated abstract: Vagus nerve stimulation is emerging as a new electroceutical therapy for treating gastric disorders. MRI in rats shows that vagus nerve stimulation significantly accelerated gastric emptying by promoting the relaxation of pyloric sphincter.



Keywords

gastric emptying; magnetic resonance imaging; rat; vagus nerve stimulation

Introduction

Dysregulation of gastrointestinal (GI) function is associated with gastroparesis (1, 2), obesity (3) gastroesophageal reflux disease and other GI disorders (4). These diseases are often chronic, idiopathic, and to date, not readily mitigated by surgical, pharmaceutical, and/or dietary treatments (5). For this reason, researchers have begun to explore electrical stimulation of the vagus nerve as an alternative strategy to remedy gastric disorders (6–10).

The vagus nerve plays an important role in mediating the interaction between the central nervous system (CNS) and the gut. It carries coordinated afferent information from the GI tract to the nucleus tractus solitarius (NTS) in the brainstem, and issues efferent signals from the dorsal motor nucleus of the vagus (DMV), primarily to the lower third of the esophagus and the stomach to modulate their functions (11–14). Different branches of the vagus innervate different parts of the GI tract. Therefore, fiber-selective or feedback-controlled stimulation of the vagus is potentially a favorable and effective approach to treat targeted gastric disorders.

Substantial efforts have been made in mapping the topographical and functional organization of the vagus nerve (15, 16). Initial promise of VNS has also been demonstrated for treating epilepsy (17), anxiety disorders (18), chronic heart failure (19), apnea (20) and inflammation (21). However, the therapeutic potential of VNS on gastric disorders remains unclear and its mechanism-of-action is still elusive. The reasons are likely multiple, but two stand out: First, the GI tract is not only innervated by the extrinsic vagovagal neurocircuits, but also by its intrinsic enteric network. The interplay of extrinsic and intrinsic innervations are rather

complex (11). Second, different gastric regions are innervated by different vagal branches, thereby having differential responses to VNS, yet proper functioning of the GI tract is thought to require a coordinated choreography of all gastric regions (15).

Most existing neuromodulation protocols measure physiological responses to stimulation at discrete locations without considering the global state of the stomach (22–24). In this regard, magnetic resonance imaging (MRI) yields simultaneous surveys of many tissues, making it an ideal tool to study various aspects of gastric motility. While gastric MRI has been increasingly applied to humans (25–27), it has rarely been used in small animal models for preclinical assessment. We recently developed a contrast-enhanced animal MRI technique for comprehensive assessment of gastric anatomy, motility, emptying and nutrient absorption in small animals (28). Adopting this technique, we set out to evaluate the effects of cervical VNS on antral contraction, pyloric opening and gastric emptying in healthy rats. The proposed experimental protocol and findings could offer new insights in the use of animal gastric MRI to evaluate the efficacy of therapeutics in treating gastric disorders.

Materials and Methods

Briefly, a gadolinium-based contrast agent was mixed with the animal's meal in order for chyme to appear "bright" in MRI scans, thereby delineating the gastric and intestinal volume. A multi-slice MRI sequence was used to scan the GI volume with high spatial resolution, and a similar sequence with a smaller spatial coverage was used to scan antral contractions with high temporal resolution. Measurements of gastric functions and physiology included the overall change in GI volume, gastric emptying, forestomach volume, corpus volume, antral volume, antral contraction frequency, antral peristaltic wave velocity, antral contraction amplitude, pyloric opening size, intestinal filling and, indirectly, absorption.

Animal Protocol

Thirty rats (Sprague-Dawley, male, 228–330g) were included in the study. All study procedures were approved by the Purdue Animal Care and Use Committee. Rats were housed individually in ventilated cages with elevated stainless steel wire floors during all time to prevent the animals from accessing their feces. The environment was maintained on a 12:12h light-dark cycle (lights on at 6AM and lights off at 6PM).

Animal Preparation and Surgical Protocol

According to a feeding protocol described elsewhere (28), each animal was trained until (approximately 7 days) it would voluntarily consume a fixed quantity (10g) of DietGel (DietGel Recovery, ClearH2O, ME, USA). On the day for gastric MRI, each animal was given the test meal with a mixture of dietgel and an MRI contrast agent – Gadolinium (Gd). Specifically, 10g dietgel was liquefied through double-boiling in warm water at 45° C and mixed with 22.4mg Gd-DTPA powder (#381667, Sigma Aldrich, St. Louis, USA). The liquefied dietgel solution was cooled to room temperature to return it to the semi-solid gel state.

Following an over-night food restriction (18 hours, 5PM to 11AM), rats were able to voluntarily consume the Gd-labeled test meal in 14 ± 5 minutes. Then, each animal was anesthetized with 4% isoflurane mixed with oxygen at a flow rate of 500ml/min for 5 minutes. Rats were allocated into 3 groups as follows: 1) an unoperated control group including the rats that did not receive surgery (n=11); 2) a sham control group including the rats that only received sham surgery (n=9); 3) a VNS group including the rats that received both surgery and vagus nerve stimulation (n=10). Rats in the sham and VNS groups underwent the identical neck surgery for implantation of a bipolar cuff electrode around the left cervical vagus nerve.

After administering a pre-operative bolus of carprofen (10mg kg^{-1} , IP; Zoetis, NJ, USA) and performing a toe-pinch to assure adequate anesthesia, a ventral midline cervical incision was made between the mandible and sternum. Anesthesia was maintained by 2.5–3.0% isoflurane mixed with oxygen at a flow rate of 1000ml/min throughout the electrode implant and sham implant surgery. The subcutaneous tissue of the ventral neck was then bluntly dissected and retracted laterally together with the mandibular salivary glands to reveal the trachea and the left carotid artery. Upon exposure of the left carotid artery, the left cervical vagus nerve, which sits lateral and runs parallel to the carotid artery above the level of the carotid bifurcation, was identified. The connective tissues surrounding the left cervical vagus nerve were carefully dissected so that a 10–15 mm portion of the cervical vagal trunk was isolated from the carotid artery. A custom-designed bipolar cuff electrode (MicroProbes, Gaithersburg, MD, USA) with a platinum-iridium wire lead was wrapped and secured on the isolated vagus nerve. The lead was externalized prior to suturing the incision site.

The animal was then placed in prone position on a water-heated MR-compatible cradle. On the cradle, the animal received a bolus injection of 0.01mg kg^{-1} dexmedetomidine solution (0.05mg ml^{-1} , SC; Zoetis, NJ, USA). Five minutes later the isoflurane dose was reduced to 0.3–0.5% isoflurane mixed with oxygen at a flow rate of 500ml/min. Fifteen minutes after the initial bolus, a continuous subcutaneous infusion of dexmedetomidine was administered ($0.03\text{mg kg}^{-1}\text{ hour}^{-1}$, SC). An MRI-compatible system (SA Instruments Inc., Stony Brook, NY, USA) was used to monitor respiration, cardiac pulsation, and body temperature to ensure a stable physiological state throughout the experiment. The two leads of the vagal electrodes were connected to a pair of twisted wires that ran from the MRI bore to the console room, and the wires were further connected to a constant-current stimulator (A-M Systems Model 2200). Upon the start of the first MRI acquisition, electrical pulses (monophasic pulses with alternating polarity, inter-pulse duration (IPD) = 50ms; pulse amplitude (PA) = 0.6mA; pulse width (PW) = 0.36ms; frequency = 10Hz; 20 seconds on and 40 seconds off) were delivered to the cervical vagus throughout the 4-hour experiment.

Gastric MRI

The animals were scanned in a 7-tesla horizontal-bore small-animal MRI system (BioSpec 70/30; Bruker Instruments, Billerica, USA) equipped with a gradient insert (maximum gradient: 200mT m^{-1} ; maximum slew rate: $640\text{T m}^{-1}\text{ s}^{-1}$) and a volume transmit/receive ^1H RF coil (86 mm inner-diameter).

As in our earlier study (28), after the long axis of the stomach was localized with the initial MRI scans, the MRI protocol was performed with a series of alternating volumetric scans and fast scans; the former was for quantifying gastric volume with higher spatial resolution and larger spatial coverage, whereas the latter was for assessing antral motility with higher temporal resolution and more targeted spatial coverage. The volumetric scans were acquired using a two-dimensional Fast Low Angle Shot gradient echo (FLASH) sequence with repetition time (TR) = 124.131 ms, echo time (TE) = 1.364 ms, flip angle (FA) = 90°, 30 oblique slices, slice thickness = 1 mm, field of view (FOV) = 60 × 60 mm², in-plane resolution = 0.23 × 0.23 mm², and 4 averages. The fast scans were acquired using a two-dimensional FLASH sequence with TR/TE = 11.784/1.09ms, FA = 25°, four oblique slices, slice thickness = 1.5mm, FOV = 60 × 60 mm², in-plane resolution 0.47 × 0.47 mm², no averaging, and 150 repetitions. The four fast scan slices were positioned and adjusted to cover the antrum, pylorus and duodenum, based on the immediately preceding volumetric images to account for the stomach displacement during gastric emptying.

To minimize motion artifacts, both volumetric and fast scans were respiration-gated such that images were acquired during end-expiratory periods, while the chest volume stayed roughly unchanged. With the respiratory gating, the volumetric scan took about 4 minutes; the fast scan took ~2 seconds per repetition and lasted ~6 min for 150 repetitions. The volumetric and fast scans were repeated in an interleaved manner for a total of four hours.

Assessment of GI volume, compartmental volume, and emptying rate

The GI volume was assessed globally and compartmentally, which included the gastric volume and intestinal volume. The intestinal volume comprised the duodenal, jejunal, and ileal volumes. The gastric volume was further partitioned into forestomach, corpus and antral volumes. The volumes were sampled approximately every 15 minutes for 4 hours. Specifically, the contrast-enhanced luminal volumes of the GI tract at different times were segmented, partitioned, and quantified separately from the volumetric scans by using an image processing pipeline (28). Note that some voxels in large veins with much shortened T1 and those in the renal medulla due to systemic Gd absorption might be mistakenly included in the above segmentation. Such spurious voxels were manually identified and excluded from the analysis. In addition, the heterogeneous image intensity (e.g. feces with unenhanced and/or partly enhanced image intensity) in the colon raised difficulty in proper quantification of the colonic volume; hence voxels in the colon were removed as well. The processing time for a 4-hour volumetric dataset was about 1.5 hours. The volume of each compartment measured at intervals was further normalized as a percent of its initial volume at time 0. This normalization step allowed us to observe the relative volume change over time for each animal, while accounting for the varying amount of the meal intake and the preparation time for different animals. The time series of gastric volumes were resampled at 15-min intervals for every animal and then averaged across animals to characterize gastric emptying at the group level. Note that the VNS began at the start of the first volumetric scan (t = 0). Since the scan took about 4 minutes to acquire, a 4-minute delay was added to all time series.

Assessment of gastric motility

The frequency, amplitude and velocity of the peristaltic wave in the gastric antrum were quantified from the fast scans by using a custom-built Matlab image processing pipeline (28). Briefly, the antrum was first delineated from a stack of 4 slices, and the proximal-to-distal antral axis was determined. The cross-sectional areas perpendicular to the proximal-to-distal antral axis were then calculated by summing the number of antral voxels within each cross-sectional plane. By iteratively doing so for each volume, we obtained a time series that represented the cross-sectional area (CSA) change of the antrum at different locations distant to the pylorus. In the CSA time series, the maxima of the time series indicated antral distension and the minima antral contraction (i.e. the lumen was largely occluded by the depth of the constriction of the antral wall). The antral contraction frequency, occlusion amplitude and velocity were computed from the time series. In this study, the antral motility indices were obtained from the middle antrum, which was 4.7mm distant from the pylorus. This process was repeated for each volume. A time series that characterized the antral motility was obtained and resampled at 15-min intervals for every animal and then averaged across animals. Since VNS began at the start of the first volumetric scan ($t = 0$) and the volumetric scan and the fast scan took about 4 minutes and 6 minutes, respectively, a 10-minute delay was added to all time series. Of the 11 animals in the unoperated control group, 5 animals were excluded from the study due to either disoriented antrum or the presence of gastric air in the antrum. One animal in the VNS group was excluded from the study using the same exclusion criteria.

Measurement of the size of the pyloric sphincter lumen

To measure the size of the pyloric sphincter, we manually determined a cross-sectional plane that was perpendicular to the outflow direction of the terminal antrum on the segmented GI tract from the volumetric scans. The CSA of the pyloric sphincter was calculated by counting the number of luminal voxels in the determined plane, as shown in Fig. 3A. This process was repeated for each volume, and a time series that characterized the pyloric opening was obtained for each animal. The time series were resampled at 15-min intervals for every animal and then averaged across animals for analysis at the group level. A 4-minute delay was added to all time series for the same reason mentioned in the gastric emptying analysis.

Statistical analysis

Unless otherwise stated, all data are reported as mean \pm standard error of mean (SEM). A probability (p-value) < 0.05 was considered significant to reject the null hypothesis. To evaluate the significance of the difference in the gastric emptying profile between the two conditions, the emptying curve from each subject was modeled by a Weibull distribution expressed as below, for which the two parameters (t_{const} β) were estimated by the least-squares method (29),

$$V(t)(\%) = 100 \exp \left[- \left(\frac{t}{t_{const}} \right)^\beta \right]$$

where $V(t)$ is the remaining volume at experiment time t (min), β is the shape parameter of the curve, and t_{const} is the emptying time constant (min). The fitting was done by using the *fit* function in MATLAB. Only the estimated parameters with goodness of fit (R^2) metrics greater than 0.85 were subject to the subsequent statistical analysis. One-way ANOVA was performed to assess the significance of the differences between the fitted parameters for the unoperated control, the sham control, and the VNS conditions, followed by Fisher's least significant difference (LSD) post hoc tests. To further assess the difference of the remaining volume in each compartment, one-way ANOVA with LSD test was conducted on individual time points between the three conditions. One-way ANOVA with LSD test was also applied to determine whether there were statistically significant differences in antral motility indices and the degree of the pyloric opening between the three conditions.

Results

Gd-labeled meal revealed the gastric lumen in MRI

All animals voluntarily consumed the Gd-labeled Dietgel on the day of imaging following 7 days of training. Specifically, the unoperated control rats consumed 6.90 ± 0.40 g meal in 14 ± 5 minutes; the sham rats consumed 8.45 ± 0.43 g meal in 15 ± 3 minutes; the VNS rats consumed 8.62 ± 0.59 g meal in 13 ± 7 minutes. The overall preparation time (the interval between the finish of eating and the start of the first MRI acquisition) for the unoperated control rats, the sham rats and the VNS rats was 22 ± 7 minutes, 83 ± 15 minutes and 75 ± 10 minutes, respectively. Eleven unoperated control rats were scanned for gastric MRI under low dose anesthesia; Nine sham rats were scanned for gastric MRI after sham surgical operations, whereas the remaining 10 rats were scanned with their left cervical vagus nerve being electrically stimulated for 4 hours after the surgery (Fig. 1A). Figure 1B shows the electrical stimulation paradigm. Adding gadolinium to the meal shortened the T1 relaxation. The meal thus appeared with much higher image intensity on the T1-weighted images compared to the surrounding tissues (Fig. 1C, 1D). The gastric volume and motility were quantified according to our previously established image processing pipeline (28). Animals that underwent acute electrode implant surgeries prior to imaging were euthanized at the end of the experiment.

Vagus nerve stimulation promoted gastric emptying

Fig. 2 shows the modulatory effect of VNS on gastric emptying. All volumes were normalized against the volume within each respective GI compartment at time 0 – which indicates the emptying rate with respect to their initial volume – and then averaged across animals. Fig. 2A illustrates the 3D GI tract rendered from the high resolution volumetric scans. Different compartments of the GI tract were separated and labeled by the processing pipeline. Fig. 2B shows the volume change (%) of the GI tract (gastric volume + intestinal volume). The volume changes in the GI tract is strictly determined by the meal volume, secretion volume, and the volume absorbed by the intestines. In the first 30 minutes, there was an increase in the total GI volume in the unoperated control group (likely due to secretion) but not in the sham and the VNS groups. After approximately one hour, the rate of volume change was faster in both sham group and VNS group than in the unoperated control group. Although no significant difference in total GI volume change was found between the

sham group and the VNS group, gastric emptying was significantly faster with VNS compared to the sham condition (Fig. 2C). A compartment-wise analysis showed that the emptying rate in the forestomach (Fig. 2E) and corpus (Fig. 2F) was increased by VNS but not in the antrum (Fig. 2G). Note that the antral volume stayed almost unchanged in the unoperated control condition, suggesting a balance between secretion, the delivery of chyme to the antrum and the transfer of chyme to the duodenum. Such a balance was not observed in the sham and VNS condition. In Fig. 2D, the intestinal volume (i.e., duodenum, jejunum and ileum) increased as the chyme filled the intestines, especially during the first 60 minutes. The intestinal filling rate was greater with VNS than in the sham condition, consistent with the accompanying difference in gastric emptying rate. The intestinal volume stayed roughly unchanged from 60–240 minutes, which suggests a balance between intestinal filling and absorption.

The gastric emptying curves were quantitatively characterized by a shape constant (β) and a time constant (t_{const}). No significant difference in shape constant was found between the three conditions [unoperated control (n=8) vs. sham (n=9) vs. VNS (n=9): 1.08 ± 0.22 vs. 0.80 ± 0.09 vs. 0.89 ± 0.10]. The time constant [unoperated control (n=6) vs. sham (n=9) vs. VNS (n=9): 822.2 ± 134.8 vs. 1011.9 ± 134.0 vs. 437.1 ± 40.7 minutes] was significantly less in the VNS condition than in the sham condition ($p < 0.05$), suggesting that VNS increased the rate of gastric emptying. No significant difference in time constant was found between the unoperated control group and the sham group ($p = 0.2419$). The differences of volume change within each compartment were also statistically evaluated as illustrated in Fig. 2B–G. Specifically, there was a significant difference between the sham and the VNS group in the overall (i.e. 4-hour) volume change in the stomach (sham vs. VNS: $29.1 \pm 1.5\%$ vs. $40.7 \pm 3.9\%$, $p < 0.05$), in the corpus (sham vs. VNS: $14.7 \pm 8.8\%$ vs. $43.2 \pm 7.9\%$, $p < 0.05$), and a non-significant difference in the forestomach (sham vs. VNS: $30.3 \pm 2.1\%$ vs. $37.6 \pm 3.0\%$, $p = 0.14$). A significant difference in volume change was also found between the unoperated control and the sham group in the total GI volume and the antral volume ($p < 0.05$).

Vagus nerve stimulation increased the size of the pyloric lumen

The luminal CSA of the pyloric ring was defined as shown in Fig. 3A. Figure 3B shows how the size of the pylorus size changed during the 4-hour experiment for VNS animals and their controls. With VNS, the luminal CSA of the pylorus was on average significantly greater than that without VNS (sham vs. VNS: 1.5 ± 0.1 vs. 2.6 ± 0.4 mm²; $p < 0.05$; Fig. 3C), particularly at $t = 4, 19, 34, 79, 169$ and 184 minutes ($p < 0.05$). The increase in the pyloric luminal size was further correlated with the increase in stomach emptying. The overall volume change (%; four-hour difference) in the stomach was significantly correlated with the CSA of the pyloric lumen ($r = 0.5887$, $p < 0.001$). Note that VNS in general led to a larger volume change in the stomach and to a greater size of the pylorus as shown in Fig. 3D.

Vagus nerve stimulation promoted antral motility

Next, we examined whether VNS modulated antral motility in terms of the frequency, amplitude and velocity of antral contractions. When sampled every ~2 seconds, the contrast-enhanced gastric MRI captured the gastric motility as a wave of antral contraction

propagating along the long axis of the antrum. We found that surgical operations resulted in a non-significant decrease in antral contraction amplitude (unoperated control vs. sham: 30.6 ± 3.0 vs. 23.3 ± 3.0 percent occlusion; $p=0.1667$; Fig. 4B) and a significant decrease in the propagating velocity of contraction waves (unoperated control vs. sham: 0.67 ± 0.03 vs. 0.50 ± 0.02 mm/s; $p<0.05$; Fig. 4C). With VNS, the antral contraction amplitude was on average significantly greater than the sham condition (sham vs. VNS: 23.3 ± 3.0 vs. 32.5 ± 3.0 percentage occlusion; $p<0.05$; Fig. 3B, right panel), particularly during the first two hours of the experiment (Fig. 3B, left panel). Similarly, the propagating velocity of contraction waves was on average significantly greater with VNS than without VNS (sham vs. VNS: 0.50 ± 0.02 vs. 0.67 ± 0.03 mm²; $p<0.05$; Fig. 3C, right) throughout the 4-hour experiment. However, no significant differences were found in contraction frequency between the three conditions (unoperated control vs. sham vs. VNS: 6.3 ± 0.1 vs. 6.1 ± 0.2 vs. 6.4 ± 0.2 cpm; $p=0.4482$; Fig. 3A, right panel), except that differences were found during the first 30 minutes and the last 30 minutes of the experiment ($p<0.05$; Fig. 3A, left panel).

Discussion

Here, we used a contrast-enhanced MRI protocol to assess the effects of VNS on gastric motility and emptying in rats. We developed an effective feeding protocol in which animals voluntarily consume a Gd-labeled meal, circumventing the need of oral gavage. The Gd-labeled meal, which could be adopted for human applications, allowed gastrointestinal organs to be clearly defined. The present paradigm makes it possible to non-invasively track how the GI tract handles a voluntarily taken Gd-labeled test meal by measuring total gastric and even regional stomach emptying, antral motility (i.e., frequency, amplitude and velocity), the extent of pyloric opening, and intestinal filling.

Stimulation of the left cervical vagus nerve with the selected parameters was found to significantly enhance the rate of gastric emptying by a factor of ~ 1.4 . The increased emptying rate was found to relate to the tonic relaxation or dilation of the pyloric sphincter, as VNS significantly enlarged the pyloric luminal CSA (or equivalently reduced its tone). Surgical operation of electrode implantation on the vagal nerve was found to cause a confounding reduction in antral contraction amplitude and velocity. However, VNS significantly promoted antral contraction amplitude and velocity as compared to its sham controls. Although antral hypomotility was observed in the sham rats, no significant difference in gastric emptying was found between the unoperated control rats and the sham control rats. Therefore, the degree to which the pyloric ring opens appears to be the primary contributor to the increase in gastric emptying. In sum, the experimental protocol used in this work opens an avenue for non-invasive assessment of the efficacies of neuromodulation protocols that might be used for further tuning and optimizing stimulation parameters in the future.

Effect of vagus nerve stimulation on gastric emptying

A major finding in this study was that VNS promoted gastric emptying by increasing pyloric relaxation or opening. Two accepted driving forces pace gastric emptying. The first driving force is the transient transpyloric flow generated by antral contraction, where the peristaltic

on antral motility. Our results showed that surgical operations [e.g. injection of carprofen, manipulation of vagal nerve and a higher dose (2.5–3.0%) of isoflurane used during the surgery] compromised antral contraction amplitude and velocity, whereas VNS turned out to promote antral contraction amplitude and velocity back to a level similar (or more) to those observed in the unoperated control rats. The antral hypomotility was most likely due to the use of analgesic agent and anesthesia (43, 44). Nevertheless, we do not rule out the possibility that manipulating the vagal nerve (i.e. mechanical stimulation) during the surgery could also have an impact on antral motility.

It is not surprising that the frequency of antral contraction remains virtually unchanged. Intrinsic gastric pace-setter potential (associated with the interstitial cells of Cajal network) sets the basic electrical rhythm (BER) of the contractions in mono-gastric animals, whereas the level of vagal discharge influences the amplitude and propagating velocity of the contractions (45, 46). The VNS settings used in this study resulted in different effects on the pyloric sphincter and the gastric antrum. The same settings relaxed the pyloric sphincter but imposed an excitatory effect on the gastric antrum, resulting in an increased strength and a higher propagating velocity of the antral contractions. The positive correlation between the amplitude and the propagating velocity of antral contractions is consistent with recent findings based on slow wave recordings in humans (47). We speculate that stimulation at the cervical vagus may release different neurotransmitters at different terminals of gastric vagal branches. However, additional investigations, for instance, stimulating at different gastric vagal branches, will be required to disentangle the effect of VNS on different gastric regions.

The responses of gastric motility to VNS may also be attributed to the specific pattern of stimulation employed. Grundy et al. showed that efferent stimulation in bursts (10 times faster for one-tenth of the time as the constant frequency stimulation) elicited significantly greater antral contractions than with a constant frequency (i.e., the same pattern as we used in this study) in the ferret antrum (23). Speculatively, the main difference between these two types of stimulation is that when stimulating at continuous frequency, both excitatory and inhibitory pathway are activated, and the latter may overshadow the former effect. However, when stimulating at bursts, successive post-synaptic events are likely superimposed due to temporal summation of the fast-delivered electrical pulses, therefore resulting in a dominating acetylcholine output within the enteric plexus that could elicit stronger antral contractions.

Naturalistic feeding protocol and non-invasive imaging ensures undisturbed vagovagal reflex

A noteworthy feature of this study is that the animals were trained to voluntarily consume the test meal. Naturalistic food ingestion allows for interaction between meal and oral mucosa to properly activate cognitive and sensory processing in the brain (48, 49). These processes presumably take place in the brainstem as well as higher brain areas (e.g., amygdala), thereby supplying synaptic input to modulate the DMV neurons that control the vagal outflow to the gut. Further, meal-associated, swallow-induced esophageal distention activates vagovagal reflexes, thus triggering receptive relaxation of the forestomach and the corpus. Receptive relaxation allows the expansion of the gastric reservoir to accommodate

the ingesta with minimal change of intra-gastric pressure (50). In contrast, oral gavage typically introduces stress (51, 52). In addition, artificial delivery (i.e., oral gavage) of the food directly to the stomach bypasses vagovagal reflexes and increases intra-gastric pressure (53).

This study highlights the capability of animal gastric MRI in assessing physiological functions of the stomach. In-vivo assessment of natural GI functions in small animals is more challenging given their smaller body size, much faster gastric motility, and the need for voluntary meal consumption. Existing methods are often invasive (or even lethal) (54), radioactive (55) and indirect (56), or employ other imaging methods (57) that offer limited spatial, temporal, or quantitative resolution. For example, the gastric barostat method requires intubation of a balloon in the proximal or distal stomach to measure gastric motility. Such invasive intubation in fact acts like a bolus, which could be physiologically confounding and greatly interrupts vagal innervation to the gut. Another example is ultrasound, which allows for non-invasive imaging of the gastric reservoir (57). However, ultrasound images possess limited spatial resolution and their image quality are typically degraded by speckles. The use of ultrasound in quantifying gastric functions is technically cumbersome, and the analysis is labor intensive and often observer dependent. Lastly, radioactive imaging (i.e., gastric scintigraphy) has been mainly applied to quantify gastric volumes, but the inability of repeated measurements and the relatively low sampling rate limits its use in simultaneous assessment of contractile motility. In summary, MRI overcomes the above-mentioned challenges and provides a unique opportunity to assess the gastric response to therapeutic treatments without perturbing the ongoing and spontaneous physiology. More importantly, recent advances in standardizing experimental protocols and developing computer-assisted software for processing gastric MRI data have made gastric MRI increasingly accessible to research and clinical practices (28, 58–60).

Acknowledgments

This work was supported in part by NIH SPARC 1OT2TR001965 and Purdue University. Authors have no conflict of interest.

References

1. Parkman HP, Hasler WL, Fisher RS. American Gastroenterological Association technical review on the diagnosis and treatment of gastroparesis. *Gastroenterology*. 2004; 127:1592–1622. [PubMed: 15521026]
2. Patrick A, Epstein O. Review article: gastroparesis. *Alimentary Pharmacology & Therapeutics*. 2008; 27:724–740. [PubMed: 18248660]
3. Woods S, Seeley R. Understanding the physiology of obesity: review of recent developments in obesity research. *International Journal of Obesity & Related Metabolic Disorders*. 2002;26.
4. El-Serag HB. Time trends of gastroesophageal reflux disease: a systematic review. *Clinical Gastroenterology and Hepatology*. 2007; 5:17–26. [PubMed: 17142109]
5. Abell T, Bernstein VK, Cutts T, et al. Treatment of gastroparesis: a multidisciplinary clinical review. *Neurogastroenterology & Motility*. 2006; 18:263–283. [PubMed: 16553582]
6. Camilleri M, Toouli J, Herrera M, et al. Intra-abdominal vagal blocking (VBLOC therapy): clinical results with a new implantable medical device. *Surgery*. 2008; 143:723–731. [PubMed: 18549888]

7. Sarr MG, Billington CJ, Brancatisano R, et al. The EMPOWER study: randomized, prospective, double-blind, multicenter trial of vagal blockade to induce weight loss in morbid obesity. *Obesity surgery*. 2012; 22:1771–1782. [PubMed: 22956251]
8. McCallum RW, Sarosiek I, Parkman H, et al. Gastric electrical stimulation with Enterra therapy improves symptoms of idiopathic gastroparesis. *Neurogastroenterology & Motility*. 2013; 25:815. [PubMed: 23895180]
9. Andrews PL, Sanger GJ. Abdominal vagal afferent neurones: an important target for the treatment of gastrointestinal dysfunction. *Current opinion in pharmacology*. 2002; 2:650–656. [PubMed: 12482726]
10. Sinclair R, Bajekal RR. Vagal nerve stimulation and reflux. *Anesthesia & Analgesia*. 2007; 105:884–885.
11. Travagli RA, Anselmi L. Vagal neurocircuitry and its influence on gastric motility. *Nature Reviews Gastroenterology & Hepatology*. 2016; 13:389–401. [PubMed: 27251213]
12. Travagli RA, Hermann GE, Browning KN, Rogers RC. Musings on the Wanderer: What's New in our Understanding of Vago-Vagal Reflexes?: III. Activity-dependent plasticity in vago-vagal reflexes controlling the stomach. *American journal of physiology Gastrointestinal and liver physiology*. 2003; 284:G180. [PubMed: 12529266]
13. Qin C, Sun Y, Chen J, Foreman RD. Gastric electrical stimulation modulates neuronal activity in nucleus tractus solitarii in rats. *Autonomic Neuroscience*. 2005; 119:1–8. [PubMed: 15893702]
14. Liu J, Qiao X, Chen JZ. Vagal afferent is involved in short-pulse gastric electrical stimulation in rats. *Digestive diseases and sciences*. 2004; 49:729–737. [PubMed: 15259491]
15. Precht JC, Powley TL. The fiber composition of the abdominal vagus of the rat. *Anatomy and embryology*. 1990; 181:101–115. [PubMed: 2327594]
16. Berthoud H, Carlson N, Powley T. Topography of efferent vagal innervation of the rat gastrointestinal tract. *American Journal of Physiology-Regulatory, Integrative and Comparative Physiology*. 1991; 260:R200–R207.
17. Ben-Menachem E. Vagus-nerve stimulation for the treatment of epilepsy. *The Lancet Neurology*. 2002; 1:477–482. [PubMed: 12849332]
18. George MS, Sackeim HA, Rush AJ, et al. Vagus nerve stimulation: a new tool for brain research and therapy. *Biological psychiatry*. 2000; 47:287–295. [PubMed: 10686263]
19. De Ferrari GM, Crijns HJ, Borggrefe M, et al. Chronic vagus nerve stimulation: a new and promising therapeutic approach for chronic heart failure. *European heart journal*. 2010; 32:847–855. [PubMed: 21030409]
20. Malow B, Edwards J, Marzec M, Sagher O, Fromes G. Effects of vagus nerve stimulation on respiration during sleep A pilot study. *Neurology*. 2000; 55:1450–1454. [PubMed: 11094096]
21. de Jonge WJ, van der Zanden EP, Bijlsma MF, et al. Stimulation of the vagus nerve attenuates macrophage activation by activating the Jak2-STAT3 signaling pathway. *Nature immunology*. 2005; 6:844–851. [PubMed: 16025117]
22. Martinson J. The effect of graded stimulation of efferent vagal nerve fibres on gastric motility. *Acta Physiologica*. 1964; 62:256–262.
23. Grundy D, Scratcherd T. Effect of stimulation of the vagus nerve in bursts on gastric acid secretion and motility in the anaesthetized ferret. *The Journal of physiology*. 1982; 333:451–461. [PubMed: 7182473]
24. Eagon J, Kelly K. Effect of electrical stimulation on gastric electrical activity, motility and emptying. *Neurogastroenterology & Motility*. 1995; 7:39–45. [PubMed: 7627865]
25. Curcic J, Sauter M, Schwizer W, Fried M, Boesiger P, Steingoetter A. Validation of a golden angle radial sequence (GOLD) for abdominal T1 mapping during free breathing: Demonstrating clinical feasibility for quantifying gastric secretion and emptying. *Journal of Magnetic Resonance Imaging*. 2015; 41:157–164. [PubMed: 24391022]
26. Menys A, Taylor SA, Emmanuel A, et al. Global small bowel motility: assessment with dynamic MR imaging. *Radiology*. 2013; 269:443–450. [PubMed: 23801770]
27. Hoad C, Parker H, Hudders N, et al. Measurement of gastric meal and secretion volumes using magnetic resonance imaging. *Physics in Medicine & Biology*. 2015; 60:1367. [PubMed: 25592405]

28. Lu K-H, Cao J, Oleson S, Powley TL, Liu Z. Contrast Enhanced Magnetic Resonance Imaging of Gastric Emptying and Motility in Rats. *IEEE Transactions on Biomedical Engineering*. 2017; 64:2546–2554. [PubMed: 28796602]
29. Locatelli I, Mrhar A, Bogataj M. Gastric emptying of pellets under fasting conditions: a mathematical model. *Pharmaceutical research*. 2009; 26:1607–1617. [PubMed: 19337822]
30. Gleysteen JJ, Gohlke EG. The antrum can control gastric emptying of liquid meals. *Journal of Surgical Research*. 1979; 26:381–391. [PubMed: 431056]
31. Stemper T. Gastric emptying and its relationship to antral contractile activity. *Gastroenterology*. 1975; 69:649–653. [PubMed: 1158083]
32. Strunz UT, Grossman MI. Effect of intragastric pressure on gastric emptying and secretion. *American Journal of Physiology-Endocrinology And Metabolism*. 1978; 235:E552.
33. Kelly KA. Gastric emptying of liquids and solids: roles of proximal and distal stomach. *American Journal of Physiology-Gastrointestinal and Liver Physiology*. 1980; 239:G71–G76.
34. Ehrlein H. Inductographic studies on the pyloric sphincter. *Communications in Soil Science and Plant Analysis*. 1992; 1008:493–493.
35. Edin R, Ahlman H, Kewenter J. The vagal control of the feline pyloric sphincter. *Acta Physiologica*. 1979; 107:169–174.
36. Edin R. The vagal control of the pyloric motor function: a physiological and immunohistochemical study in cat and man. *Acta physiologica Scandinavica Supplementum*. 1980; 485:1–30. [PubMed: 6163319]
37. Mir SS, Telford GL, Mason GR, Ormsbee HS. Noncholinergic nonadrenergic inhibitory innervation of the canine pylorus. *Gastroenterology*. 1979; 76:1443–1448. [PubMed: 437443]
38. Malbert C, Mathis C, Laplace J. Vagal control of pyloric resistance. *American Journal of Physiology-Gastrointestinal and Liver Physiology*. 1995; 269:G558–G569.
39. Takahashi T, Owyang C. Vagal control of nitric oxide and vasoactive intestinal polypeptide release in the regulation of gastric relaxation in rat. *The Journal of Physiology*. 1995; 484:481–492. [PubMed: 7602539]
40. Martinson J. Vagal Relaxation of the Stomach Experimental Re-investigation of the Concept of the Transmission Mechanism. *Acta Physiologica*. 1965; 64:453–462.
41. Martinson J, Muren A. Excitatory and inhibitory effects of vagus stimulation on gastric motility in the cat. *Acta Physiologica*. 1963; 57:309–316.
42. Allescher H, Daniel E, Dent J, Fox J, Kostolanska F. Extrinsic and intrinsic neural control of pyloric sphincter pressure in the dog. *The Journal of physiology*. 1988; 401:17–38. [PubMed: 2902218]
43. Torjman MC, Joseph JJ, Munsick C, Morishita M, Grunwald Z. Effects of isoflurane on gastrointestinal motility after brief exposure in rats. *International journal of pharmaceuticals*. 2005; 294:65–71. [PubMed: 15814231]
44. Ailiani A, Neuberger T, Brasseur J, et al. Quantifying the effects of inactin vs Isoflurane anesthesia on gastrointestinal motility in rats using dynamic magnetic resonance imaging and spatio-temporal maps. *Neurogastroenterology & Motility*. 2014; 26:1477–1486. [PubMed: 25257924]
45. Szurszewski JH. Modulation of smooth muscle by nervous activity: a review and a hypothesis. *Federation proceedings*. 1977:2456–2461. [PubMed: 196945]
46. Miolan J-P, Roman C. Discharge of efferent vagal fibers supplying gastric antrum: indirect study by nerve suture technique. *American Journal of Physiology-Endocrinology and Metabolism*. 1978; 235:E366.
47. Wang TH, Du P, Angeli T, et al. Relationships between gastric slow wave frequency, velocity, and extracellular amplitude studied by a joint experimental-theoretical approach. *Neurogastroenterology & Motility*. 2018:30.
48. Bonnichsen M, Dragsted N, Hansen AK. The welfare impact of gavaging laboratory rats. *ANIMAL WELFARE-POTTERS BAR THEN WHEATHAMPSTEAD-*. 2005; 14:223.
49. Brown AP, Dinger N, Levine BS. Stress produced by gavage administration in the rat. *Journal of the American Association for Laboratory Animal Science*. 2000; 39:17–21.

50. Rogers R, Hermann G, Travagli R. Brainstem pathways responsible for oesophageal control of gastric motility and tone in the rat. *The Journal of Physiology*. 1999; 514:369–383. [PubMed: 9852320]
51. Stengel A, Taché Y. Neuroendocrine control of the gut during stress: corticotropin-releasing factor signaling pathways in the spotlight. *Annual review of physiology*. 2009; 71:219–239.
52. Zheng J, Dobner A, Babygirija R, Ludwig K, Takahashi T. Effects of repeated restraint stress on gastric motility in rats. *American Journal of Physiology-Regulatory, Integrative and Comparative Physiology*. 2009; 296:R1358–R1365.
53. Damsch S, Eichenbaum G, Tonelli A, et al. Gavage-related reflux in rats: identification, pathogenesis, and toxicological implications. *Toxicologic pathology*. 2011; 39:348–360. [PubMed: 21422261]
54. Uchida M, Iwamoto C. Influence of amino acids on gastric adaptive relaxation (accommodation) in rats as evaluated with a barostat. *Journal of Smooth Muscle Research*. 2016; 52:56–65. [PubMed: 27558952]
55. Jordi J, Verrey F, Lutz TA. Simultaneous assessment of gastric emptying and secretion in rats by a novel computed tomography-based method. *American Journal of Physiology-Gastrointestinal and Liver Physiology*. 2014; 306:G173–G182. [PubMed: 24264048]
56. Uchida M, Kobayashi O, Saito C. Correlation Between Gastric Emptying and Gastric Adaptive Relaxation Influenced by Amino Acids. *Journal of neurogastroenterology and motility*. 2017; 23:400. [PubMed: 28335103]
57. Gilja O, Hausken T, Wilhelmsen I, Berstad A. Impaired accommodation of proximal stomach to a meal in functional dyspepsia. *Digestive diseases and sciences*. 1996; 41:689–696. [PubMed: 8674389]
58. Bickelhaupt S, Froehlich JM, Cattin R, et al. Software-supported evaluation of gastric motility in MRI: A feasibility study. *Journal of medical imaging and radiation oncology*. 2014; 58:11–17. [PubMed: 24131557]
59. Banerjee S, Dixit S, Fox M, Pal A. Validation of a rapid, semiautomatic image analysis tool for measurement of gastric accommodation and emptying by magnetic resonance imaging. *American Journal of Physiology-Gastrointestinal and Liver Physiology*. 2014; 308:G652–G663. [PubMed: 25540229]
60. Bharucha AE, Karwoski RA, Fidler J, et al. Comparison of manual and semiautomated techniques for analyzing gastric volumes with MRI in humans. *American Journal of Physiology-Gastrointestinal and Liver Physiology*. 2014; 307:G582–G587. [PubMed: 25012844]

Key Points

1. Vagus nerve stimulation is emerging as a new electroceutical therapy for treating gastric disorders. However, its underlying mechanism(s) and therapeutic effect(s) remain incompletely understood.
2. Vagus nerve stimulation significantly accelerated gastric emptying by promoting the relaxation of the pyloric sphincter.
3. MRI offers high spatial and temporal resolution to non-invasively characterize gastric motility and physiology in preclinical animal models.

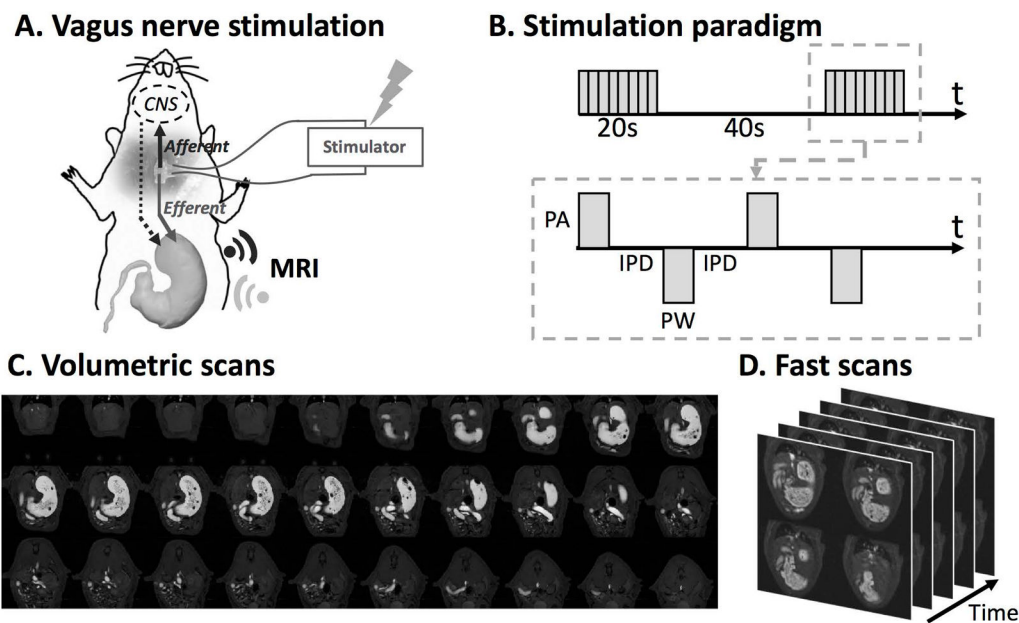


Figure 1. Vagus nerve stimulation and imaging sequence

A. Schematic diagram of the experiment protocol. A bipolar cuff electrode was implanted at the left cervical vagus of a rat. Vagus nerve stimulation was performed during the 4-hour MRI scans. **B.** Stimulation waveform, paradigm and parameters used in this study. (inter-pulse duration (IPD) = 50ms; pulse amplitude (PA) = 0.6mA; pulse width (PW) = 0.36ms; frequency = 10Hz; 20 seconds on and 40 seconds off) **C.** Example semi-coronal view images from the 2D multi-slice volumetric scan. The gastrointestinal tract is highlighted by the Gadolinium-labeled meal. **D.** Fast scans of the antrum with four slices. The position of the slice package was determined from images acquired from the volumetric scan.

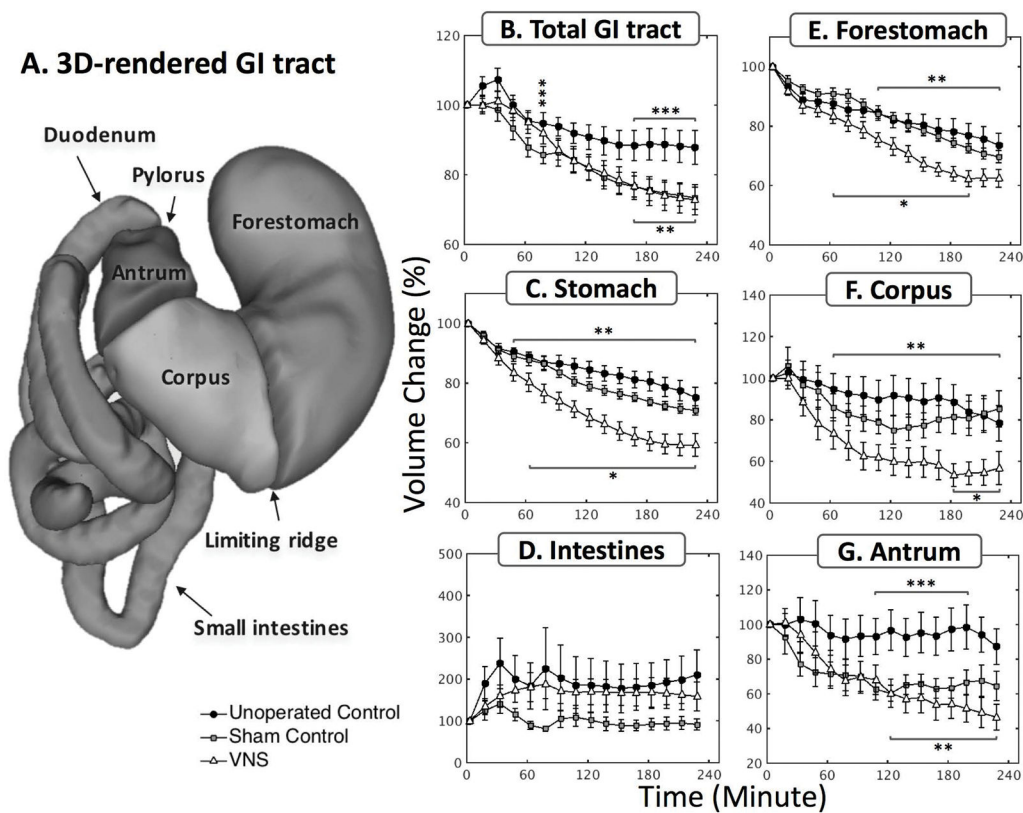


Figure 2. Vagal stimulation significantly enhances the rate of gastric emptying
A. 3D volume rendering of the lumen of the gastrointestinal tract. The profiles of volume change were quantified at a global scale including **B.** total GI tract, **C.** stomach, **D.** intestines, as well as at a compartment-wise scale including **E.** forestomach, **F.** corpus, **G.** antrum. *: $p < 0.05$: sham vs. VNS, **: $p < 0.05$: unoperated control vs. VNS, *** $p < 0.05$: unoperated control vs. sham.

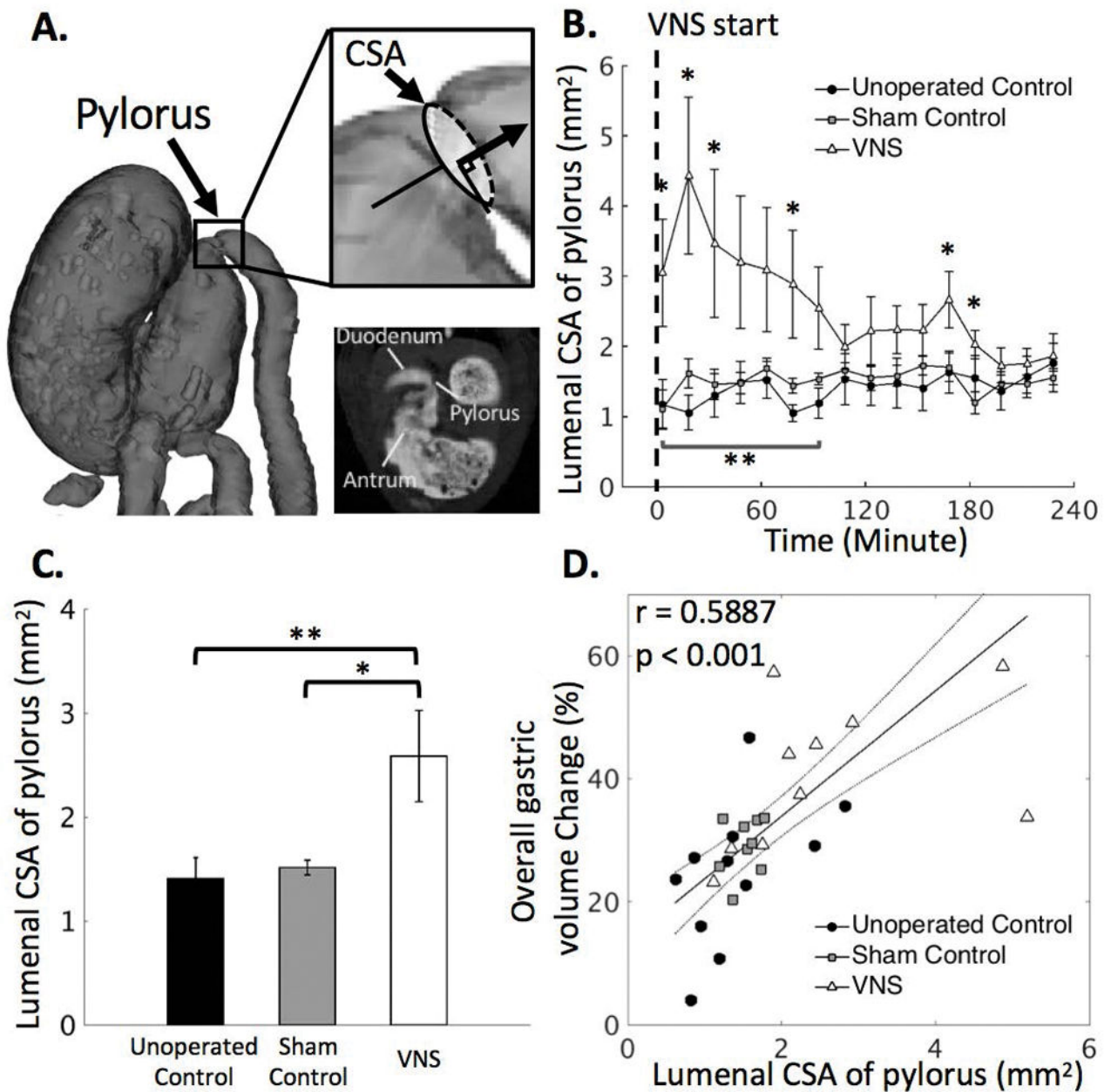


Figure 3. Quantification of the extent to which the pyloric ring opened under unoperated control, sham and VNS conditions

A. Illustrates the location of the pylorus from a 2D slice and from a rotated 3D rendered volume. The degree to which the pyloric ring opened was measured in terms of the cross-sectional area (CSA) of the luminal content in the pyloric canal from the high spatial resolution scans. **B.** The CSA of the pyloric ring is on average greater with VNS than without VNS, with notable and significant differences during the first 1 hour of the experiment. **C.** In general, VNS significantly increases the size of the pylorus. **D.** The overall gastric volume change (%; four-hour difference) is significantly correlated to the CSA of the pyloric ring. Noted that VNS in general leads to a larger volume change in the

stomach and to a greater CSA of the pyloric ring. *: $p < 0.05$: sham vs. VNS, **: $p < 0.05$: unoperated control vs. VNS, *** $p < 0.05$: unoperated control vs. sham.

Author Manuscript

Author Manuscript

Author Manuscript

Author Manuscript

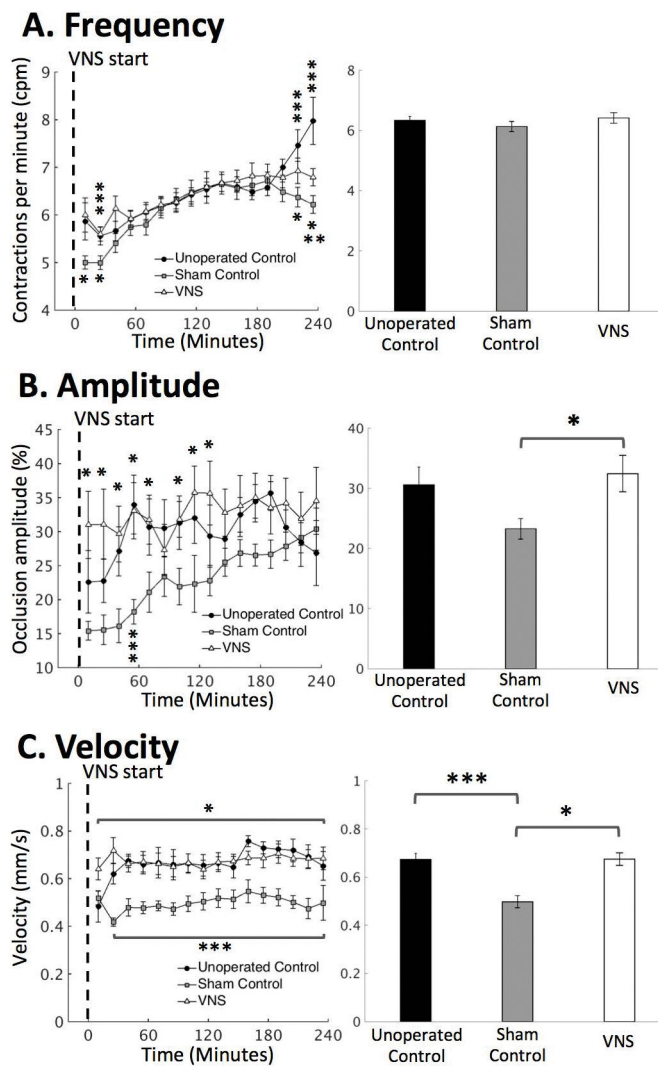


Figure 4. Quantification of antral motility under unoperated control, sham and VNS conditions Antral motility was characterized as both time series and the mean over time. **A.** Antral contraction frequency. **B.** Antral contraction amplitude. **C.** Propagating velocity of antral contraction waves. *: $p < 0.05$: sham vs. VNS, **: $p < 0.05$: unoperated control vs. VNS, *** $p < 0.05$: unoperated control vs. sham.